THE ASTRONOMICAL JOURNAL VOLUME 105, NUMBER 4 APRIL 1993

THE OCCULTATION OF GAMMA GEMINORUM BY THE ASTEROID 381 MYRRHA

ISAO SATO
The Graduate University for Advanced Studies, National Astronomical Observatory, Mitaka, Tokyo 181, Japan
MITSURU SÔMA
National Astronomical Observatory, Mitaka, Tokyo 181, Japan
TOSHIO HIROSE
International Occultation Timing Association, 1-1-13, Shimomaruko, Ota-ku, Tokyo 146, Japan
Received 1992 August 17; revised 1992 November 12

ABSTRACT

The occultation of γ Geminorum by asteroid 381 Myrrha on 1991 January 13, observed in Japan and China, was the brightest event ever seen of a stellar occultation by an asteroid. By the analysis of the timing data of this event measured in Japan, it is shown that the cross section of Myrrha is well fitted with an ellipse of $(147.2\pm2.4)\text{km}\times(126.6\pm7.9)\text{km}$. An upper limit of the diameter of γ Geminorum is also estimated to be 2.6 milliarcsec. The companion of γ Geminorum of about 7.5 mag was sited at separation (64 ± 8) milliarcsec in the direction $P=129°\pm59°$, and the relative position of Myrrha to γ Geminorum was determined to an accuracy of about 1 milliarcsec. Direct constraints on Myrrha's three-dimensional shape and the direction of its rotation axis are obtained on the assumption of it being a triaxial ellipsoid with isotropic orientation.

1. INTRODUCTION

A stellar occultation by an asteroid offers an excellent opportunity to obtain high quality information on the size, shape, rotation, and the existence of satellites of the asteroid. Many stellar occultations by asteroids have been observed since the first observation in 1958 (Millis & Dunham 1989). The brightest event previously observed had been the occultation of 3.5 mag γ Ceti by 6 Hebe on 1977 March 5. The occultation of 1.9 mag γ Geminorum (Alhena=FK5 251) by 381 Myrrha described in this paper establishes a new record.

Prior to this event in 1991 January, only two successful visual observations of asteroidal occultations had ever been made from Japan. One is the occultation of +25°1937 by 106 Dione on 1983 January 19 (cf. Kristensen 1984), and the other is that of AG+40°783 by 324 Bamberga on 1987 December 8, (Millis *et al.* 1989).

Since asteroidal occultation tracks are poorly predicted, a well-organized network encompassing all available observers over a wide area is necessary to secure adequate coverage. As a result of the cooperation of many participants in Japan, we are able to reveal here the principal characteristics of this little-studied asteroid. A large national campaign was organized in China which resulted in more than 5000 people participating in watching γ Geminorum. At least four observers recognized the event in Shandong Province but we have not received the details (Dunham 1991).

Many favorable aspects helped the present Myrrha event to be observed successfully in Japan. The occulted star was visible to the naked eye, the occultation track passed directly over the densely populated Tokyo area, the event occurred at 9 o'clock on a Sunday evening, and it was clear over a broad area along the occultation track.

Previously, Myrrha had never been the subject of detailed observation, either by photometry or by occultation (Lagerkvift *et al.* 1987, 1988). Only its mean diameter had been determined to be (124 ± 4) km by *IRAS* infrared observations (Tedesco 1989). Therefore, careful, accurate, and detailed observations of this event were expected to offer an important opportunity to obtain information on the shape and rotation of Myrrha. Actually we could obtain, as shall be shown in Secs. 3 and 4, direct constraints not only on its cross section, but on its three-dimensional shape and the orientation of its axes.

γ Geminorum is known to be a spectroscopic binary. Since it can neither be occulted by the moon nor be detected by speckle interferometry, no direct information on its companion had been obtained. During the occultation of the primary star in this event, the companion was directly observed, and its brightness and position could be determined (Sec. 5). Also, an upper limit on the angular diameter of the primary star is presented in Sec. 5 by using the photoelectric observation of the event.

2. PREDICTION AND OBSERVATIONS

Because an initial prediction of an asteroidal occultation has a considerable error, typically amounting to 1000 km, it is desirable to observe the precise relative position between the occulted star and the occulting asteroid just before the event to improve the prediction.

The initial prediction of γ Geminorum by Myrrha was made by D. W. Dunham and M. Sôma (Dunham 1990). It indicated that the event would be visible at sea to the south of Japan as shown in Fig. 1, and in China. In order to improve this prediction, a photographic observation was

 0004-6256/93/041553-09$00.90

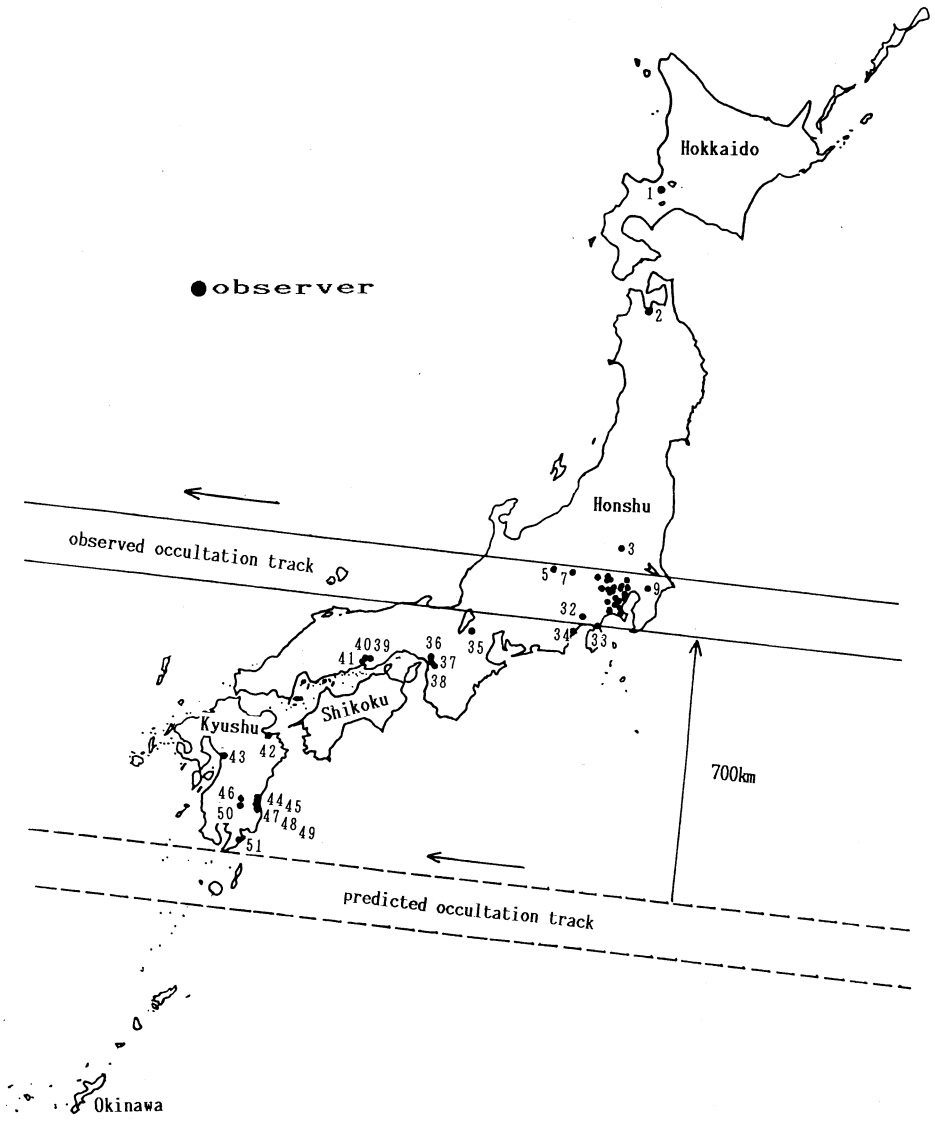

FIG. 1. The predicted and observed occultation tracks of γ Geminorum by 381 Myrrha on 1991 January 13. The best available astrometric observation indicated a path to the south of Kyushu, but many observed the shadow passing over Tokyo about 700 km north of the predicted path. This large inaccuracy mainly arose because the latest astrometric observation was made one month before the event.

made at Van Vleck Observatory on 1990 December 15. The result was no significant modification to the initial prediction. As this observation was made a month before the event, additional observations were requested but none were obtained.

According to the prediction we directed our requests for observation of the event mainly to observers in Kyushu, southwest part of Japan. However, the shadow of Myrrha actually passed far to north of Kyushu, crossing directly over Tokyo, one of the world's most populous metropolitan areas. The quantity of the shift was about 0.4 arcsec to north which corresponds to about 700 km on the ground. One photoelectric observation, two video observations, more than nine photographic observations, and several dozen visual observations with telescopes, binoculars, and no optical aid were achieved successfully.

The ephemeris of Myrrha and the position of γ Geminorum are given in Tables 1 and 2. The locations of the participating observers are listed in Table 3.

It is noted that precise timings of disappearance and/or reappearance at the center of primary component could be made with an accuracy of $0^s.02$ by using the photoelectric observation of K. Oya. For video observations gradual disappearance and reappearance over a few frames were recorded, providing the accuracy to several thirtieths of a

TABLE 1. Ephemeris of Myrrha.

0^h TD 1991	R.Asc. J2000.0	Dec. J2000.0	R.Asc. Apparent	Dec. Apparent	r	Δ	Elong.
	h m s	° ′ ″	h m s	° ′ ″	AU	AU	°
Jan. 11	6 39 40.7050	+16 14 59.204	6 39 12.1852	+16 15 30.974	3.524591	2.558720	167.1
12	6 38 53.1536	16 18 33.855	6 38 24.6191	16 19 04.983	3.524190	2.561181	166.1
13	6 38 06.0261	16 22 09.884	6 37 37.4878	16 22 40.390	3.523786	2.563947	165.1
14	6 37 19.3679	16 25 47.185	6 36 50.8258	16 26 17.092	3.523379	2.567017	164.0
15	6 36 33.2239	16 29 25.651	6 36 04.6770	16 29 54.986	3.522971	2.570389	162.9
16	6 35 47.6381	16 33 05.178	6 35 19.0843	16 33 33.964	3.522560	2.574060	161.8

Notes to TABLE 1

The values in this table were obtained by numerical integration from the orbital elements given by Batrakov (1991).

TABLE 2. The FK5 Astrometric position of γ Geminorum at 12^h TD, 1991 January 13.

R. A.	Dec.
J2000.0	
$6^h37^m42^s.69824$	$+16°23'57''.8006$

second. Unguided, stationary, photographic observations are not useful for absolute timing determination, but the duration of the occultation may be reliably determined. In such photographic observations, the chord of the event was too short to be useful if the focal length of the lens was shorter than 500 mm.

Finally, all the observations are adopted in the later analysis if the timing accuracy is expected to be either equal to or better than 1 s. The adopted observations are given in Table 4, where the observations of duration timing only are also included.

3. CROSS SECTION OF MYRRHA

In general, the shape of an asteroid is assumed to be a triaxial ellipsoid or a more irregular shape. Most of the cross sections of the asteroids obtained from the stellar occultations so far are well-fitted by ellipses if the diameter of the asteroid is larger than 100 km. Hence it is appropriate to assume that the cross section of Myrrha can be fitted with an ellipse.

Generally, an ellipse is specified with five parameters: the position of center, the lengths of major and minor axes, and the orientation angle of major axis. In this paper we determine these parameters by least-square fitting, with each observation properly weighted according to the observation method and its circumstances. In the case of observations of duration timings only, the central times of the events are also treated as unknowns to be determined by least-square fitting.

The cross section of Myrrha is found to be well-fitted by

TABLE 3. Sites of observers (Tokyo datum).

No.	Name	Observer	Longitude (East)	Latitude (North)	Height	Instrument	Method	Time Keeping
1	Sapporo, Hakkaido	O. Watanabe	141° 21′ 11.6″	42° 58′ 47.0″	110 m			
2	Aomori City, Aomori	S. Odagiri	140 48 01	40 49 31	4	7×50 B	v.	
3	Tochigi City, Tochigi	T. Hasegawa	139 37 30	36 28 00				
4	Higashimatsuyama, Saitama	K. Tanaka	139 25	36 01	60	f=400mm	v. & pg.	
5	Matsumoto, Nagano	Y. Ban	137 58 24.7	36 10 34.8		6cm R DF	pg.	
6	Sakado, Saitama	M. Komuro & N. Muto	139 22 52	35 58 20	25	NE		SW
7	Matsubarako, Nagano	H. Shibuya	138 26 16.7	36 03 26.3	1285	20cm N	v..EE	JJY
8	Chichibu, Saitama	A. Hashimoto	139 02 52	35 58 27	140	7.5cm R	v. & pg.	SW
9	Sakura, Chiba	S. Kaneko	140 11 39	35 43 50	59	15cm N	v..key tap	JJY
10	Soka, Saitama	S. Hosoi	139 47 41	35 48 14	3	finder	v.	
11	Katsushika, Tokyo	S. Waku	139 52 39.0	35 44 51.1	2	NE	v.	WWVH
12	Nerima, Tokyo	H. Karasaki	139 40 12.8	35 44 13.7	45	20cm SC	video	tel.
13	Fujimi, Nagano	K. Shima	138 18 27	35 53 25	1040	f=300mmF2.8	pg.	
14	Toshima, Tokyo	Y. Imai	139 43.4	35 43.5		NE		
15	Kodaira, Tokyo	Y. Suzuki	139 29 13.2	35 42 57.5	77	B	v.	
16	Musashino, Tokyo	K. Kitazaki	139 33 52.8	35 42 25.6	59	7.6cm R	video monitor	SW
17	Meguro, Tokyo	Astron. Club Univ. of Tokyo	139 41.2	35 39.5		NE		
18	Meguro, Tokyo	I. Sato	139 41 25.7	35 39 13.7	45	6.5cm R ex.	pg.	
						finder	v.	JJY
19	Mitaka, Tokyo	M. Sōma	139 32 11.8	35 40 26.1	59	NE		watch
20	Fuchu, Tokyo	M. Sato & T. Homma	139 28 38	35 39 17	45		video	
21	Hachioji, Tokyo	H. Koyama	139 21 36.2	35 39 30.6	133	NE	voice rec.	JJY
22	Ota, Tokyo	T. Hirose	139 41 17.8	35 34 15.6	11	NE		watch
23	Yokohama, Kanagawa	Y. Moriya	139 31 57.3	35 34 40.9	78	NE		watch
24	Machida, Tokyo	S. Fukushima	139 28 12.4	35 31 47.4		6cm R	v.	
25	Yamato, Kanagawa	A. Suzuki	139 27 43.3	35 31 03.2	87	6.5cm R DF	pg.	
26	Aikawa, Kanagawa	M. Sugai	139 18 26.0	35 30 47.7	130	f=150mmF4.0	pg.	tel.
27	Yokohama, Kanagawa	M. Yamada	139 32.6	35 27.3		NE		SW
28	Zama, Kanagawa	T. Kiyokawa	139 24 54.5	35 29 55.9	79	10cm N	v.	
29	Chigasaki, Kanagawa	K. Oya	139 24 48	35 22 12		18cm C	pe.	
30	Chigasaki, Kanagawa	Y. Hirose	139 26 07.76	35 21 51.89		f=300mmF2.8	pg.	
						B	v.	
31	Zushi, Kanagawa	H. Hayashi	139 36 30	35 17 48		B	v.	
32	Fujinomiya, Shizuoka	Y. Suenaga	138 36 38	35 11 56		f=75mm	pg.	
33	Ohito, Shizuoka	J. Horiuchi	138 57 30	35 01 18		10cm N	v.	
34	Shizuoka City, Shizuoka	W. Kakei	138 25 30	34 59 36			v.	
35	Yokaichi, Shiga	M. Ida	136 12 34.9	35 05 54.0	140	NE		
36	Suita, Osaka	S. Watanabe	135 31 40	34 47 13	24	7×50 B	v.	
37	Osaka City, Osaka	Y. Fujiwara	135 29 13.8	34 43 54.3	0		I.I.+video	JJY
38	Habikino, Osaka	M. Ueda	135 38 11	34 32 04	45		I.I.+video	
39	Okayama City, Okayama	N. Okura	133 52 36	34 36 25		18cm C	pe.	
40	Funaho, Okayama	H. Akazawa	133 42 43.3	34 34 42.6		20cm SC	pe.	
41	Kurashiki, Okayama	O. Oshima	133 40 24.4	34 32 16.4		20cm C	pe.	
42	Oita City, Oita	K. Mato	131 39 23.6	33 14 46.7	3			
43	Kumamoto City, Kumamoto	Kumamoto Civil Observatory	130 42	32 47				
44	Miyazaki City, Miyazaki	Y. Hattori & Y. Torihara	131 25 03	31 58 00			v.	
45	Miyazaki City, Miyazaki	T. Akiyoshi	131 27 08	31 55 18			v.	
46	Kobayashi, Miyazaki	T. Tomoda	130 55	31 59			v.	
47	Kiyotake, Miyazaki	K. Maeda	131 23 19	31 51 16	15		video	
48	Kiyotake, Miyazaki	Astron. Club Univ. of Miyazaki	131 22 13	31 52 13		B	pg.+v.	
49	Kiyotake, Miyazaki	Astron. Club Univ. of Miyazaki	131 21 51	31 46 58		B	pg.+v.	
50	Takasaki, Miyazaki	J. Minobe	131 04	31 51			v.	
51	ISAS, Uchinoura, Kagoshima	M. Eiraku	131 04 02.59	31 13 43.72	229	10cm R	video	

Notes to TABLE 3

R: refractive, N: Newtonian, C: Cassegrain, SC: Schmit-Cassegrain, B: binocular, NE: naked eyes DF: direct focus, ex.: extented v.: visual, pg.: photographic, pe.: photoelectric, I.I.: image intensifier, EE: eye and ear tel.: telephone time service, SW: stopwatch Observers not listed in Table 4 reported no occultation. Shifts from the Tokyo Datum to 1984 World Geodetic System are $\Delta u = -146.3$ m, $\Delta v = +507.1$ m, $\Delta w = +681.0$ m.

TABLE 4. Timings of the event.

No.	Observer	Disappearance UTC	Reappearance UTC	Adoption (*)	Time-Shift	Notes
		h m s s	h m s s		s	
3	T. Hasegawa	no occultation		A		
4	K. Tanaka	2 seconds duration		R		
5	Y. Ban	11 59 58.2 ±0.5	12 00 03.2 ±0.5	D	+0.7	companion visible
6	M. Komuro & N. Muto	11 59 59.89−0.5	12 00 12.98−0.1	RR		
7	H. Shibuya	11 59 56.1 ±0.4	12 00 02.1 ±0.5	AA	—	companion visible
8	A. Hashimoto	11 59 53 ±1.0	11 59 59 ±1.0	AA	—	companion visible
9	S. Kaneko	11 59 45.7 ±0.3	11 59 53.9 ±0.3	AA	—	primary star
			11 59 47.1 ±0.3	A	—	companion star
10	S. Hosoi	occulted		R		
11	S. Waku	11 59 47.3 ±0.3	11 59 55.9 ±0.2	AA	—	
12	H. Karasaki	11 59 48.07±0.05	11 59 57.03±0.05	AA	—	
13	K. Shima	11 59 50.6 ±0.5	11 59 59.1 ±0.5	D	+4.7	
14	Y. Imai	occulted		R		
15	Y. Suzuki	no occultation		R		
16	K. Kitazaki	11 59 54.5 ±0.8	11 59 57.7 ±0.2	RA	—	
17	Astron. Club Tokyo Univ.	occulted		R		
18	I. Sato	11 59 48.0 ±0.7	11 59 56.7 ±0.5	AA	—	primary star
			11 59 49.3 ±0.3	A	—	companion star
19	M. Sôma	11 59 49 ±1.0	11 59 58 ±1.0	AA	—	
20	M. Sato & T. Homma	11 59 48.8 ±0.1	11 59 57.7 ±0.1	AA	—	
21	H. Koyama	11 59 49.7 ±0.5	11 59 58.4 ±0.4	AA	—	
22	T. Hirose	11 59 50 ±5	11 59 55 ±5	RR		
23	Y. Moriya	11 59 52 ±2	11 59 58 ±1	RR		
24	S. Fukushima	11 59 50	12 00 00	D	−1.6	companion visible
25	A. Suzuki	11 59 46 ±1	11 59 55 ±1	D	+2.9	
26	M. Sugai	11 59 45.6 ±0.5	11 59 54.6 ±0.5	D	+4.1	
27	M. Yamada	11 59 48	11 59 53	RR		
28	T. Kiyokawa	11 59 52.4 ±0.7	11 59 58.9 ±0.4	RR		
29	K. Oya	11 59 49.12±0.02	11 59 58.00±0.02	AA	—	image reconstruction
30	Y. Hirose	11 59 48	11 59 57	D	+0.9	companion visible
31	H. Hayashi	longer than 5 seconds duration		R		
32	Y. Suenaga	11 59 59.7 ±1	12 00 05.1 ±1	D	−4.9	
33	J. Horiuchi	11 59 55.0	11 59 55.5	D	+0.4	
34	W. Kakei	no occultation		A		

Notes to TABLE 4

'Time-shift' is the correction to the reported times obtained from this analysis. Times given are reported times, not corrected.

(*) AA: both disappearance and reappearance adopted,
RA: reappearance only adopted,
RR: both disappearance and reappearance rejected,
D : duration only adopted,
A : adopted,
R : rejected.

TABLE 5. Astrometric position and motion of Myrrha.

Epoch TD	R.Asc. J2000.0	Motion per minute	Dec. J2000.0	Motion per minute
1991 Jan. 13 $12^h\,00^m$	$6^h\,37^m\,42^s.63681 \pm 5$	+0^s.032402	+16° 23′ 58″.8728 ± 12	+0″.15091

Notes to TABLE 5

The values of the motion are calculated ones from the ephemeris of Table 1.

an ellipse with axes (147.2±2.4)km×(126.6±7.9)km, and having its major axis at the position angle of 94°±10° (Fig. 2). Note that the size of the ellipse is somewhat larger than the mean diameter of (124±4)km determined by *IRAS* (Tedesco 1989).

It is also noted that the two visual observations contributing to the northern part of the ellipse, made independently by H. Shibuya and A. Hashimoto, suggest concavities or departure below the elliptical shape in that region. The southern part of the profile is constrained heavily by the photoelectric observation and by the grazing observation.

As the results of the least-square fitting described above, the relative position of Myrrha to γ Geminorum is obtained at 12^h00^m TD, 1991 January 13, with an accuracy of 1.3 km in right ascension and 2.3 km in declination, that is 0.7 milliarcsec and 1.2 milliarcsec, respectively (Table 5). This high precision almost equals that achieved by the VLBI technique. Since γ Geminorum is an FK5 star (Fricke *et al.* 1988) whose positional error in the FK5

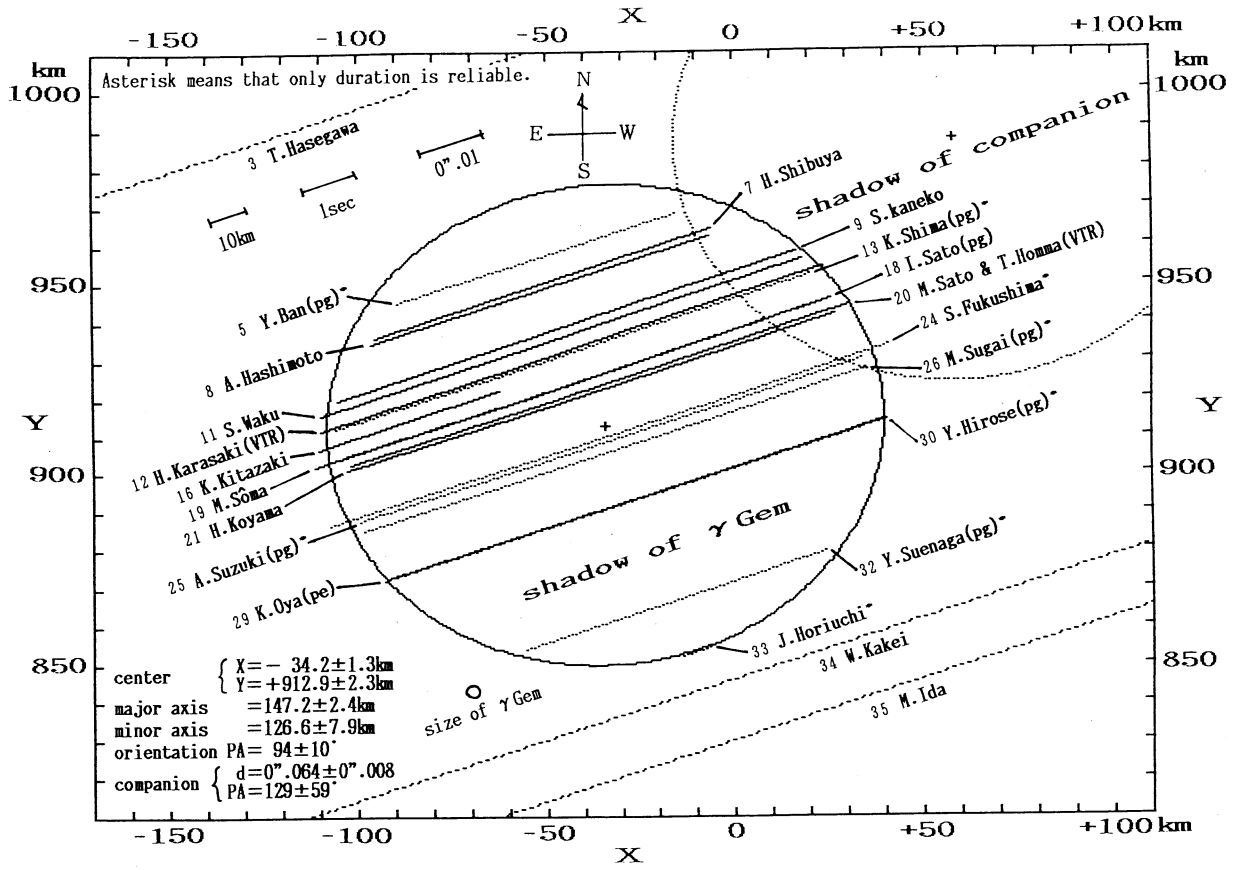

FIG. 2. The cross section of 381 Myrrha obtained by the occultation observation of γ Geminorum. The elliptical profile is fitted by weighted least squares. There may be concavity in the northern part of the ellipse. Since no observation was made near the northern limit, the accuracy of the estimated length of the minor axis is less than that of the major axis.

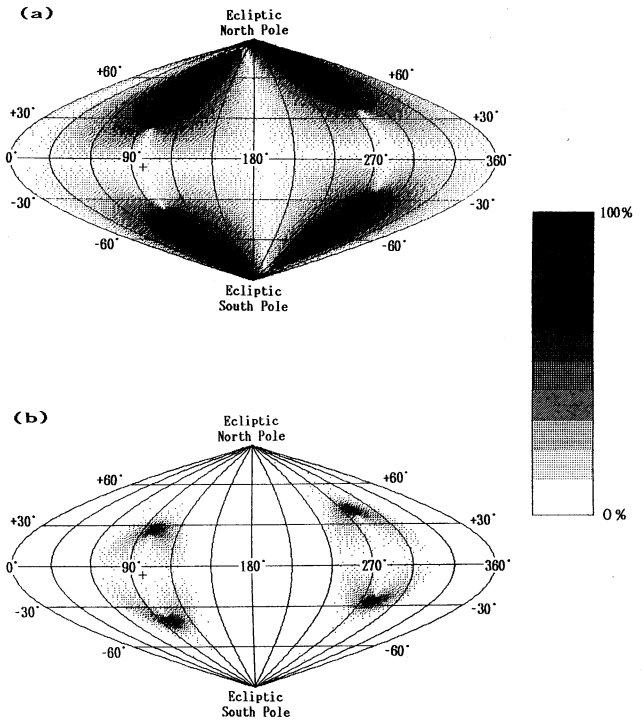

FIG. 3. The maps of the probability of the direction of the shortest principal axis of Myrrha in equal area Sanson projections. The position of γ Geminorum is $\lambda = 99\overset{\circ}{.}1$, $\beta = -6\overset{\circ}{.}7$, which is marked as "+". The density of dots indicates the range of the possible phase angle for each direction of the shortest principal axis. (a) is the geometrically constrained case and (b) is the *IRAS*-observation constrained case. Quarto symmetric distribution can be seen. *IRAS* observation constrains the direction of the shortest principal axis into the four small regions.

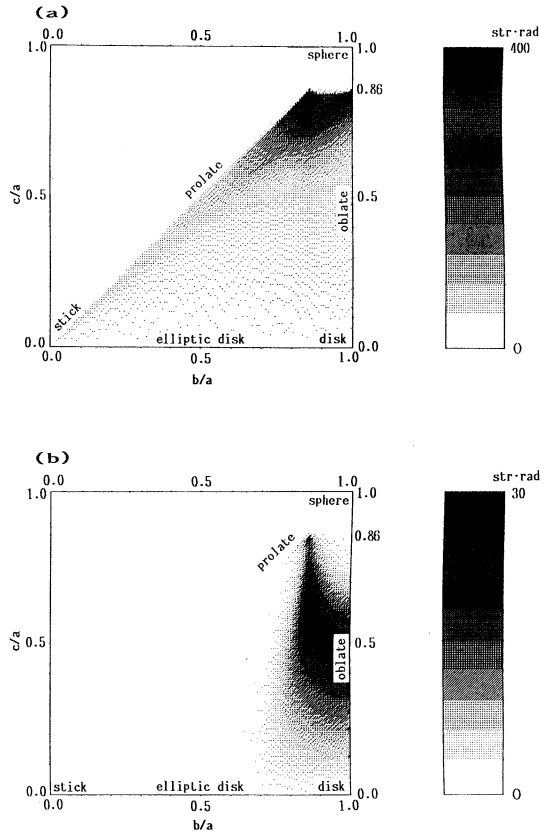

FIG. 4. The probability distributions of the axial length ratios of the three-dimensional shape of Myrrha. (a) is that of the geometrically possible shape, and (b) is that of the *IRAS*-observation constrained shape. The density of dots on the maps indicates the measure of probability. The axial length ratio of the ellipse of the observed cross section of Myrrha is 0.86. The possible region is trapezoidal. It is found from (a) and (b) that c/a should be less than 0.86 and from (b) that b/a may be greater than 0.7 by *IRAS* observation constraint.

system must be small, it is assumed in Table 5 that almost all of the corrections to the relative position is attributed to that of Myrrha.

4. DEDUCTION OF THE THREE-DIMENSIONAL SHAPE

No earlier stellar occultation by Myrrha has been observed, nor is anything known about its rotation (Magnusson 1989). The cross section of Myrrha obtained in the previous section will provide the basic constraints on the possible three-dimensional shape and the orientation of Myrrha. The shape of most asteroids greater than 100 km in its diameter are well approximated by triaxial ellipsoids. So we assume here that the three-dimensional shape of Myrrha is a triaxial ellipsoid.

As is shown in the Appendix, it is possible to derive two-dimensional probability maps of the orientation of a triaxial ellipsoid by assuming isotropic orientation from three observables, the lengths of the major and minor axes, and the orientation of the major axis of the projected elliptical cross section of the ellipsoid. We can also derive the probability for a given axial ratio among the three axes of the ellipsoid to be realized. The only parameter to derive those probabilities is the phase angle of the rotation.

Figure 3 indicates the probability maps of the direction of the shortest principal axis of the ellipsoid of Myrrha in equal area Sanson projections. We assume the rotation axis is coincident with the shortest principal axis. Figure 3(a) is the geometrically constrained case and Fig. 3(b) is the case combined with *IRAS* observation. The density of the dots indicates the range of the possible rotation phase in the direction of the rotation axis, for example, 100% means that there exists a triaxial ellipsoid solution for any phase angle between 0 to 2π radian. The direction of γ Geminorum is marked as "+." Quarto symmetry can be seen. It is found that 23.6% of all orientations have possible solutions in Fig. 3(a) but only 2.07% in Fig. 3(b). Hence the mean diameter of (124 ± 4)km obtained by *IRAS* observation gives a very strong constraint for the probability of the direction of the shortest principal axis.

The probability distributions of the axial length ratios of the three-dimensional shape of Myrrha are shown in Fig. 4. Figure 4(a) is the probability distribution of geometrically possible shapes, and Fig. 4(b) is that of *IRAS*-mean-diameter-constrained shapes. In each of Fig. 4, b/a and c/a, respectively, stand for the ratios of the length of the intermediate principal axis and the shortest principal axis

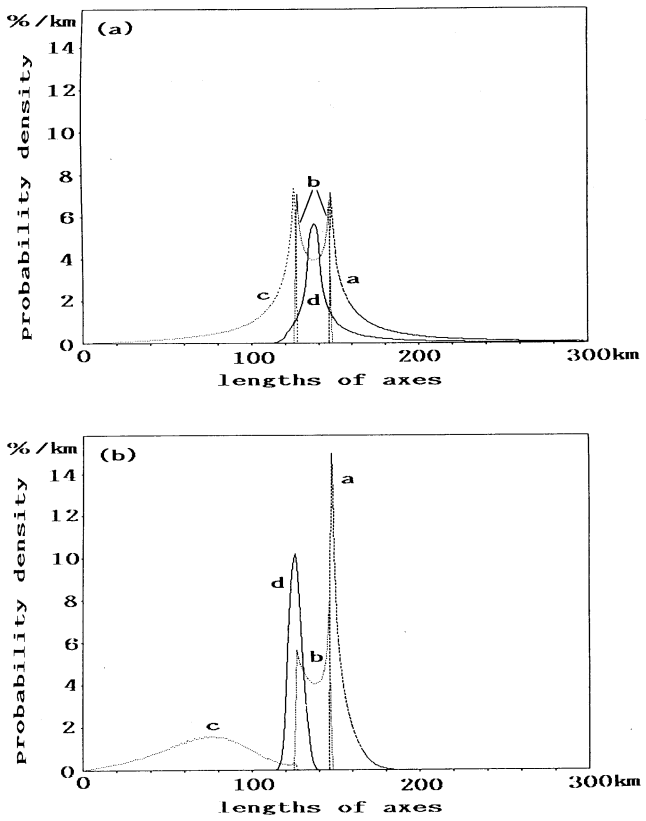

FIG. 5. The probability distribution of the lengths of the three principal axes *a*, *b*, *c* and the mean diameter *d* of the three-dimensional shape of Myrrha. (a) is the geometrically constrained case and (b) is the *IRAS* mean diameter constrained case. The constraint is found to be $c \leqslant 126.6$ km$\leqslant b \leqslant 147.2$ km$\leqslant a$ and $d \geqslant 112.1$ km. The *IRAS* observation constraint suggests that the shortest principal axis must be fairly short. However, that is unlikely.

to that of the longest principal axis. Note that the axial length ratio of the ellipse of the observed cross section of Myrrha is 0.86 and the possible region is trapezoidal as shown in Fig. 4. It is found from Figs. 4(a) and 4(b) that it is impossible, not measure zero, for Myrrha to have a more spherical shape than the ellipse of cross section, i.e., c/a should be less than 0.86. We also see from Fig. 4(b) that b/a may be greater than 0.7 by the *IRAS*-observation constraint.

The probability distributions of the lengths of three principal axes *a*, *b*, *c* and the mean diameter *d* of Myrrha are shown in Fig. 5. Figure 5(a) is the geometrically-constrained case and Fig. 5(b) is the *IRAS*-observation-constrained case. Constraints for the lengths of three principal axes are given as $c \leqslant 126.6\text{km} \leqslant b \leqslant 147.2\text{km} \leqslant a$. Figure 5(b) indicates that the *IRAS* mean diameter of (124 $\pm$4)km requires a fairly small value of *c*. Such a short principal axis seems to be unlikely for the size of Myrrha. Hence the value of the *IRAS* mean diameter may have some systematic error.

5. DIAMETER OF γ GEMINORUM AND POSITION OF THE COMPANION

γ Geminorum is known to be a spectroscopic binary. During the present occultation by Myrrha, the companion

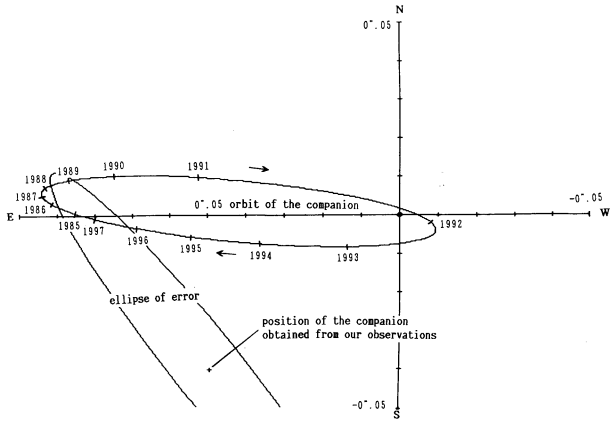

FIG. 6. The orbit of the companion by Kamper & Beardsley (1987), and the occultation observed position of the companion. Good agreement is shown for the separation from the primary star, but the position angle of the predicted position is discrepant.

was observed directly both photographically and visually while the primary was behind Myrrha. Its magnitude was about 7.5 and it was yellowish. Some observers reported that the companion was visible throughout the occultation of the primary star as shown in the Notes in Table 4. However, S. Kaneko, visually, and I. Sato, photographically (Fig. 9), reported that the companion only became visible about 1 s after the beginning of the occultation of the primary star. These observations imply that the companion was occulted earlier than the primary star. From these observations, we can estimate the distance of the companion relative to the primary star to be (64$\pm$8) milliarcsec in the direction of position angle of 129°$\pm$59°.

A set of orbital elements of the companion is derived from astrometric and spectroscopic techniques by Kamper & Beardsley (1987) and is given in their Table V. Our present observation is not consistent with the position predicted from these orbital elements; especially, a large discrepancy exists in the position angle, as is seen in Fig. 6. Although our position of the companion is based on the timings of only two observers, direct image detections by several other observers convinces us of the reliability of our result.

The photoelectric profiles observed by K. Oya show Fresnel diffraction patterns [Figs. 7(a) and 7(c)] convolved by the equipment time constant of about 200 milliseconds. As the sampling interval is 40 milliseconds, the timings of the events can be determined in the accuracy of 20 milliseconds which corresponds to 0.15 milliarcsec. Some numerical deconvolutions of the observed profile provide a reconstructed image of the occulted star [Fig. 7(b) and 7(d)]. The diameter of γ Geminorum is thus estimated to be 2.6 milliarcsec. However, the reconstructed images have damping tails, and we can only say that 2.6 milliarcsec should be regarded as an upper limit of the diameter of the primary star.

6. SUMMARY

A stellar occultation by an asteroid provides excellent information on the diameter and duplicity of the occulted

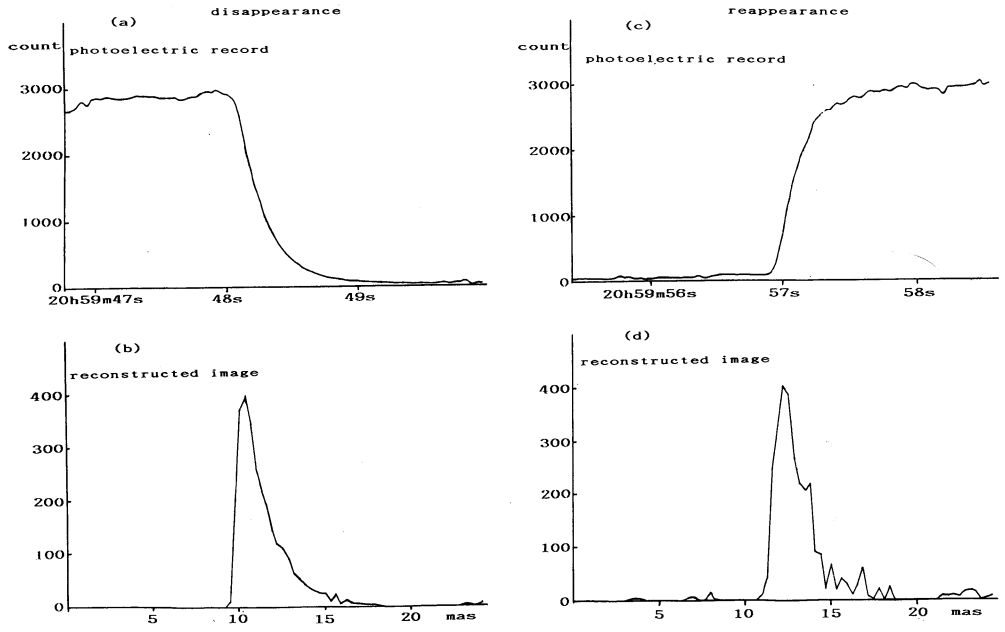

FIG. 7. The photoelectric observation recorded by K. Oya and the reconstructed image of γ Geminorum. Fresnel diffraction convolved by the equipment time constant of about 200 milliseconds produced the gradual disappearance and reappearance. From the reconstructed image of γ Geminorum, the timings of disappearance and reappearance were obtained to an accuracy of 20 milliseconds. An upper limit of the diameter of γ Geminorum is also obtained as 2.6 milliarcsec.

star, in addition to the size, shape and rotation axis of the occulting asteroid. At the occultation of γ Geminorum by Myrrha on 1991 January 13, more than 30 positive observations are obtained in Japan. Prior to this event, little was known about 381 Myrrha.

The cross section of the projected image of Myrrha is well-fitted by an ellipse of $(147.2\pm2.4)\times(126.6\pm7.9)$km with the position angle of the major axis of $94°\pm10°$. The derived size is somewhat larger than the mean diameter of (124 ± 4)km by *IRAS* infrared observation (Tedesco 1989). A highly accurate determination is made of the relative position of Myrrha with respect to γ Geminorum. The 1-milliarcsec-accuracy reported in this paper corresponds to that achieved by VLBI observations and is beyond the capabilities of the usual single optical observation.

Assuming that Myrrha is a triaxial ellipsoid, we also succeeded in obtaining some direct constraints on the three-dimensional shape and orientation of Myrrha.

Furthermore, by the analysis of the photoelectric profile of the diffraction pattern, the upper limit of the diameter of γ Geminorum is derived as 2.6 milliarcsec. The companion of γ Geminorum was directly observed for the first time during this event. The position of the companion relative to the primary star is derived at the epoch of the observation and is compared to the previous prediction.

We thank Dr. D. W. Dunham who provided us the prediction, W. Nissen who revised our manuscript, Dr. W. H. Warren who gave us a useful suggestion, Dr. M. Yoshizawa and K. Tomita for their useful discussions, and many observers who provided us their observations listed in Table 3.

APPENDIX: DERIVATION OF THREE-DIMENSIONAL SHAPE OF A TRIAXIAL ELLIPSOID FROM AN ELLIPSE OF CROSS SECTION

The apparent cross section visible from a great distance is expressed in quadratic form below:

$$1={}^t\mathbf{r}RX\,{}^tR\mathbf{r},$$

where R and X are matrices defined by the following:

$$X={}^tR_z(\theta)QR_z(\theta),$$

$$R=R_z(90°+P)R_x(90°+\delta_s)\,{}^tR_z(90°+\alpha_c-\alpha_s)\times{}^tR_y(90°-\delta_c),$$

in which Q is given by

$$Q=\begin{pmatrix}1/a^2 & 0 & 0\\ 0 & 1/b^2 & 0\\ 0 & 0 & 1/c^2\end{pmatrix},\quad (a\geqslant b\geqslant c>0),$$

where a, b, and c are the lengths of the three principal axes, and R_x, R_y, and R_z are rotation matrices around x, y, and z axes, respectively:

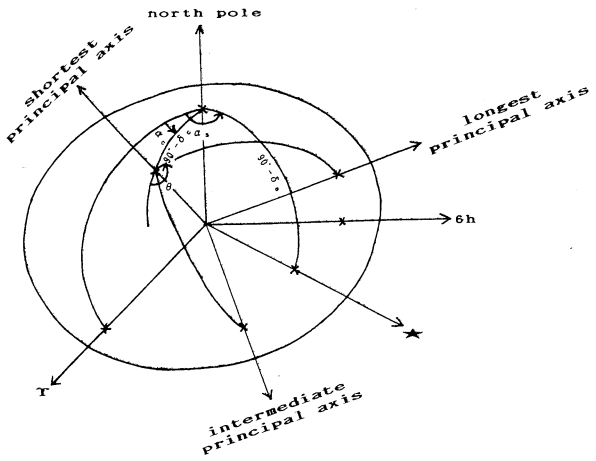

FIG. 8. Perspective view of a triaxial ellipsoid seen from the star.

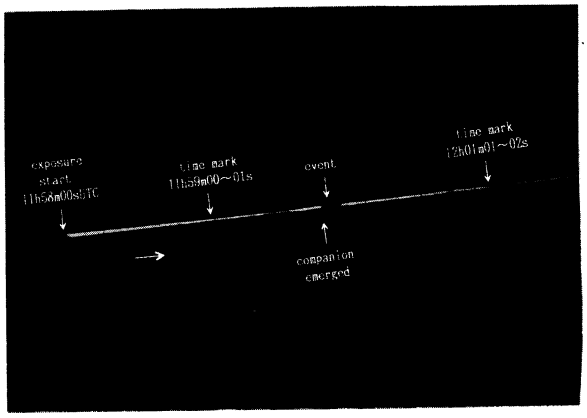

FIG. 9. The occultation of γ Geminorum by 381 Myrrha is shown as an 8.7 second interruption of the trace of diurnal motion of γ Geminorum during 4 min exposure. Thin clouds passed to dim the star several times during the exposure.

$$R_x=\begin{pmatrix}1 & 0 & 0\\ 0 & \cos\theta & \sin\theta\\ 0 & -\sin\theta & \cos\theta\end{pmatrix},$$

$$R_y=\begin{pmatrix}\cos\theta & 0 & -\sin\theta\\ 0 & 1 & 0\\ \sin\theta & 0 & \cos\theta\end{pmatrix},$$

$$R_z=\begin{pmatrix}\cos\theta & \sin\theta & 0\\ -\sin\theta & \cos\theta & 0\\ 0 & 0 & 1\end{pmatrix},$$

and $\mathbf{r}$ is a vector,

$$\mathbf{r}={}^t(x,y,z)={}^t(x_1,x_2,x_3).$$

In the above equations, α_s, δ_s are the right ascension and declination of the star, and α_c, δ_c are those of the direction of the shortest principal axis of the ellipsoid, θ is the phase angle of the longest principal axis, and P is the position angle of the major axis of the apparent ellipse, respectively, as shown in Fig. 8.

The condition that the lengths of the major and minor axes of the apparent ellipse are A and B, respectively, is resolved by Lagrange's method of indeterminate coefficient. The maximum value of the coordinate x_k is derived by maximizing the following Lagrangian form:

$$\Phi=x_k+\lambda\left(\sum_{i,j=1}^{3}K_{ij}x_ix_j-1\right),$$

where λ is an indeterminate coefficient, and K_{ij} $(i=1,2,3;\ j=1,2,3)$ are the components of $RX\,{}^tR$. The necessary condition to be maximum is

$$\frac{\partial\Phi}{\partial x_i}=\delta_{ik}+2\lambda\sum_{j=1}^{3}K_{ij}x_j=0,$$

$$\frac{\partial\Phi}{\partial\lambda}=\sum_{i,j=1}^{3}K_{ij}x_ix_j-1=0,$$

where δ_{ij} is Kronecker's delta. By solving these equations, we obtain

$$x_j=\frac{K_{kj}^{-1}}{(K_{kk}^{-1})^{1/2}},$$

hence

$$x_k=(K_{kk}^{-1})^{1/2}.$$

Therefore, the condition that the lengths of the apparent major and minor axes are A and B, respectively, is derived by substituting $K=RX\,{}^tR$:

$$(RX^{-1}\,{}^tR)_{11}=A^2,$$

$$(RX^{-1}\,{}^tR)_{22}=B^2,$$

and the cross components of K_{12} and K_{21} should be vanished because the axes of the ellipse are parallel to those of the coordinates, hence,

$$(RX^{-1}\,{}^tR)_{12}=(RX^{-1}\,{}^tR)_{21}=0.$$

In these simultaneous equations, A, B, P, α_s, δ_s are observed quantities and a, b, c, α_c, δ_c, θ are unknowns. Since there are only three equations for six unknowns, these simultaneous equations cannot be resolved unless values of three parameters are assumed. It is appropriate to assume values for α_c, δ_c, and θ, because the direction of the shortest principal axis (α_c, δ_c) is the greatest moment of inertia, in most cases. Hence, it can be regarded as the rotation axis, and it can be assumed that the rotation phase θ is uniformly probable from 0 to 2π radian. Therefore the total volume of the parameters of the orientation is $(4\pi$ str$)\times(2\pi$ rad$)$.

Suppose $D=a^2+b^2$ and $E=a^2-b^2$. Now taking D, E, and c^2 as independent parameters, then the triple simultaneous equations are reduced to the linear equations:

$$\begin{pmatrix} R_{11}^2+R_{12}^2 & (R_{11}^2-R_{12}^2)\cos 2\theta+2R_{11}R_{12}\sin 2\theta & 2R_{13}^2 \\ R_{21}^2+R_{22}^2 & (R_{21}^2-R_{22}^2)\cos 2\theta+2R_{21}R_{22}\sin 2\theta & 2R_{23}^2 \\ R_{11}R_{21}+R_{12}R_{22} & (R_{11}R_{21}-R_{12}R_{22})\cos 2\theta+(R_{11}R_{22}+R_{12}R_{21})\sin 2\theta & 2R_{13}R_{23} \end{pmatrix} \begin{pmatrix} D \\ E \\ c^2 \end{pmatrix} = \begin{pmatrix} 2A^2 \\ 2B^2 \\ 0 \end{pmatrix},$$

where

$$R_{11}=\sin\delta_c\sin(\alpha_c-\alpha_s)\sin P-[\cos\delta_c\cos\delta_s+\sin\delta_c\sin\delta_s\cos(\alpha_c-\alpha_s)]\cos P,$$
$$R_{12}=\cos(\alpha_c-\alpha_s)\sin P+\sin\delta_s\sin(\alpha_c-\alpha_s)\cos P,$$
$$R_{13}=\cos\delta_c\sin(\alpha_c-\alpha_s)\sin P+[\sin\delta_c\cos\delta_s-\cos\delta_c\sin\delta_s\cos(\alpha_c-\alpha_s)]\cos P,$$
$$R_{21}=\sin\delta_c\sin(\alpha_c-\alpha_s)\cos P+[\cos\delta_c\cos\delta_s+\sin\delta_c\sin\delta_s\cos(\alpha_c-\alpha_s)]\sin P,$$
$$R_{22}=\cos(\alpha_c-\alpha_s)\cos P-\sin\delta_s\sin(\alpha_c-\alpha_s)\sin P,$$
$$R_{23}=\cos\delta_c\sin(\alpha_c-\alpha_s)\cos P-[\sin\delta_c\cos\delta_s-\cos\delta_c\sin\delta_s\cos(\alpha_c-\alpha_s)]\sin P,$$
$$R_{31}=\cos\delta_c\sin\delta_s-\sin\delta_c\cos\delta_s\cos(\alpha_c-\alpha_s),$$
$$R_{32}=\cos\delta_s\sin(\alpha_c-\alpha_s),$$

and

$$R_{33}=-\sin\delta_c\sin\delta_s-\cos\delta_c\cos\delta_s\cos(\alpha_c-\alpha_s).$$

By solving these simultaneous equations, a, b, and c are obtained. However, any solution must also satisfy the additional condition, $a\geqslant b\geqslant c>0$. In fact, as an ellipsoid does not necessarily exist for all orientations of the ellipsoid, the orientation is constrained.

Let us define the mean diameter of an ellipsoid as

$$d=\sqrt{\frac{a^2+b^2+c^2}{3}},$$

then the expected value of the mean square diameter of the cross section equals d^2 as easily proved; i.e.,

$$E\left[\frac{A^2+B^2}{2}\right]=\frac{a^2+b^2+c^2}{3}=d^2,$$

where the integration is done over all orientations of (4π str)$\times$(2π rad) in equal measure, isotropic orientation.

The *IRAS* mean diameter of (124±4)km is interpreted in our definition. The constraint by *IRAS* observations is expressed as a Gaussian weighted distribution of $\mu=124$ km, $\sigma=4$ km.

The constraint derived above gives significant information on the rotation of the asteroid.

REFERENCES

Batrakov, Y. V. 1991, Ephemerides of Minor Planets for 1992 (Institute of Theoretical Astronomy, Leningrad)

Dunham, D. W. 1990, Occultation Newsletter 5, 38

Dunham, D. W. 1991, private communication

Fricke, W., Schwan, H., & Lederle, T. 1988, Fifth Fundamental Catalogue, Veröff Astron. Recher. Inst., Heidelberg, No. 32 (FK5)

Kamper, K. W., & Beardsley, W. R. 1987, AJ, 94, 1302

Kristensen, L. K. 1984, ANa, 305, 207

Lagerkvift, C. I., Barucci, M. A., & Capria, M. T. 1987, Asteroids Photometric Catalogue (Configlio Nazionale Delle Richerche, Roma)

Lagerkvift, C. I., Barucci, M A. & Capria, M. T. 1988, Asteroids Photometric Catalogue (Configlio Nazionale Delle Richerche, Roma)

Magnusson, P. 1989, in Asteroids II, edited by R. P. Binzel, T. Gehrels, and M. S. Matthews (The University of Arizona Press, Tucson), p. 1180

Millis, R. L., *et al.* 1989, AJ, 98, 1094

Millis, R. L., & Dunham, D. W. 1989, in Asteroids II, edited by R. P. Binzel, T. Gehrels, and M. S. Matthews (The University of Arizona Press, Tucson), p. 148

Tedesco, E. F. 1989, in Asteroids II, edited by R. P. Binzel, T. Gehrels, and M. S. Matthews (The University of Arizona Press, Tucson), p. 1090